Density functional study of oxygen migration processes for silicon quantum dots

R. J. Eyre,* J. P. Goss, and P. R. Briddon
School of Natural Sciences, Newcastle University, Newcastle Upon Tyne NE1 7RU, United Kingdom
(Received 28 September 2007; published 26 December 2007)

The migration kinetics of oxygen inserted into the surface back-bond network of hydrogen-terminated silicon quantum dots has been examined. Diffusions both inward and lateral to the surface have been modeled. We find activation energies for migration generally far exceed the thermal energy available at room temperature, and thermodynamically, the production of subsurface oxygen is not favored. Surface dangling bonds significantly affect migration barriers, stabilize subsurface threefold coordination of oxygen, and surface bridging structures that redshift the onset of optical transitions. We also show that ionization enhances oxygen migration of a fully passivated dot, but it does not favor subsurface oxygen.

DOI: 10.1103/PhysRevB.76.245325 PACS number(s): 73.22.−f, 73.21.La, 73.43.Cd, 81.16.Pr

I. INTRODUCTION

Silicon quantum dots (Si-QDs) lend themselves to application within the life sciences due to their excellent optical properties, biostability, and anticipated nontoxicity. Additionally, silicon is cheap to manufacture and widely available. Quantum confinement is key to the optical properties of quantum dots, including those made of other materials, such as cadmium selenide, but it is also clear that the role of surface chemistry is also vitally important.[1] This is particularly the case when oxidation is considered.

Many studies have reported changes in photoluminescence emission as a result of oxidation. For example, both red- and blueshifts have been observed for dots exposed to atmosphere,[2,3] with the latter also reported for systems immersed in solution for long periods of time.[4] Also, blue peaks have been observed upon oxidation in addition to the characteristic band-gap transitions.[5,6] The oxidation of silicon nanocrystals in atmosphere is self-limiting,[7,8] typically achieving self-saturation within a few of days. In addition, the diffusion of oxygen has been demonstrated to be weaker in silicon nanoparticles than for the bulk.[9]

Recently, infrared spectroscopy of silicon nanocrystals[10] produced via a nonthermal plasma of Ar and SiH_4 indicates oxidation of a hydrogen-terminated surface proceeds via insertion of oxygen into the Si—Si back bonds. These structures are much like those observed on the (111) and (100) hydrogen-terminated bulk surfaces when exposed to atomic oxygen.[11,12] Oxidation of Si-QDs in ethanol or water has also been observed indicating the formation of Si-O-Si structures.[4,13] Infrared absorption experiments involving hydrogen-terminated (111) and (100) surfaces of bulk silicon exposed to water also result in the formation of back-bonded oxygen, in this case, via a Si-OH intermediate.[14,15]

Quantum-chemical simulations have identified potential mechanisms behind optical changes observed upon the addition of oxygen. One class is made up from surface defects, such as silanone (Si═O) groups[2,16] and Si-O-Si structures.[16,17] These give rise to surface states that lie in the band gap leading to a decrease in the emission energy (a redshift). A separate process leading to an increase in the optical emission energy (the blueshift) involves the formation of SiO_2 capping layers, increasing quantum confinement.[7,8,18]

Relatively few studies have examined the energetics for the migration of oxygen from sites on the initially oxidized surface of Si-QDs. However, the viability of oxygen diffusion within the Si-QDs impacts upon increasing the quantum size effect through the growth kinetics of a SiO_2 capping layer and the stability of surface defect structures responsible for surface state optical transitions.

Of the limited computed data available, diffusion of interstitial oxygen perpendicular to the surface has been simulated using a Si_9 cluster, where some hydrogen termination was fixed to simulate a more extended network,[19] with unpassivated, hydrogen- and hydroxyl terminated surfaces considered. Inward diffusion barriers were around 1 eV higher than that in bulk silicon [$\sim$2.5 eV (experiment[20,21]) and $\sim$2.7 eV (theory[22,23])] for passivated surfaces. However, the inward diffusion is relatively easy for unpassivated surfaces at around 1 eV. Since some surface dangling bonds are present even after a hydrofluoric acid treatment,[10] the lowering of the barrier to incorporating subsurface oxygen with Si-QDs may be highly significant. Diffusion lateral to the surface of Si-QDs within the surface silicon back-bond network has received no attention in the literature to our knowledge.

In this study, we present an examination of both inward and lateral diffusions of atomic oxygen. The local surface terminations within the vicinity of the migration process have been treated for a variety of combinations of hydrogen, and hydroxyl groups, as well as surface dangling bonds.

II. METHOD

We perform density functional simulations within the generalized gradient approximation[24] implemented within the AIMPRO code (*ab initio* modeling program[25]). Core electrons are eliminated via use of norm-conserving pseudopotentials,[26] with valence wave functions being represented on each atom by combinations of Cartesian *s*, *p*, and *d* Gaussian orbitals.[27] Each Si-QD is modeled using periodic boundary conditions in a face-centered-cubic lattice with the centers of the Si-QDs separated by $\sim$2 nm. The convergence of the properties with respect to the lattice constant has been established to be less than 1 meV for the total energy differences quoted in this paper. The periodic boundary condition

 ©2007 The American Physical Society

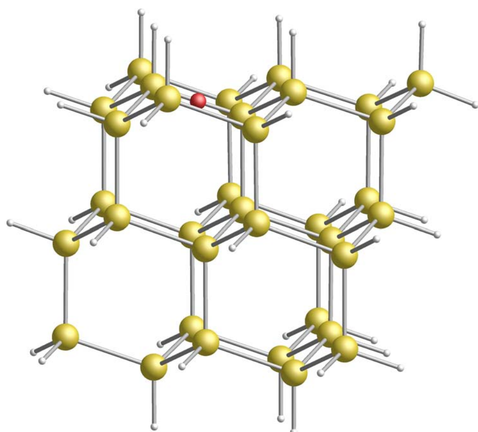

FIG. 1. (Color online) Schematic of a $Si_{35}H_{36}O$ Si-QD, with a diameter of ~1 nm. Silicon, oxygen, and terminating hydrogen atoms are shown in yellow (light gray), red (dark gray), and white, respectively. The location of the oxygen corresponds to the initial position indicated in Fig. 2.

allows the charge density to be Fourier transformed within a plane-wave basis, for which we use a cut-off energy of 300 Ry.

The basic atomic model used to represent a Si-QD is a hydrogen-terminated cluster of ~1 nm diameter ($Si_{35}H_{36}$), as shown schematically including an interstitial oxygen atom in Fig. 1. Structures are optimized using a conjugate-gradient approach, terminating with the condition that consecutive structural relaxation lower the energy by less than 1 meV. Migration barriers are determined using the well-established climbing nudged-elastic-band method,[28,29] with 13 images.

We adopt the notation that the forward activation energy for the reaction $A \rightarrow B$ is E^a, and ΔE is the change in total energy subsequent to the reaction. Thus, an exothermic reaction results in $\Delta E < 0$ and the activation energy for the reverse reaction is given by $E^a - \Delta E$.

We have considered two classes of migration process, inward to the surface and lateral within the surface, labeled (i) and (ii), respectively, in Fig. 2. For the 1 nm Si-QD, path (i) involves oxygen migrating from the surface (Fig. 1) to a Si—Si bond within the Si-QD core, whereas path (ii) results in a similar Si-O-Si structure at the surface.

In all cases, the Si-QD surface is hydrogen terminated, but with three surface sites treated differently. Two, labeled X and Y in Fig. 2, are adjacent to the migration path, and a third site, labeled Z, is located at a distance not directly bonded to silicon atoms involved in the oxygen migration. These three sites are varied in combinations of hydrogen (H), hydroxyl (OH), and dangling bonds (DBs).

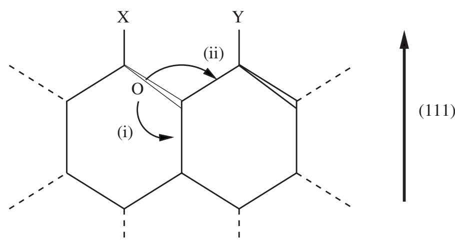

FIG. 2. A schematic of the Si-QD surface illustrating the migration paths. Paths (i) and (ii) correspond to inward and lateral processes, respectively. Variations in the local surface termination are labeled X and Y, as discussed in the text.

Due to the suspected role of charging in "blinking" during photoluminescence spectroscopy experiments,[30,31] we have also varied the charge state Q. In this context, we calculate the adiabatic ionization potential (IP) and electron affinity (EA) relative to vacuum using the highest occupied molecular orbital (HOMO) (ε_h) and lowest unoccupied molecular orbital (LUMO) ($-\varepsilon_l$), respectively. Although this approximation neglects relaxation in the charged systems, we have compared the values for IP and EA obtained in this manner against those obtained from differences in total energies and found in those fully passivated systems examined; ε_h and $-\varepsilon_l$ are good indicators for electrical transitions. Vibrational modes are calculated by obtaining second derivatives of the total energy with respect to the atom positions, using a finite difference approach, and the dynamical matrix constructed in the usual way.

Finally, optical absorption spectra are obtained using the calculated dielectric function as described elsewhere.[32] This calculation sums all transitions between filled and empty bands, with a large number of empty bands included to ensure reasonable convergence for energies in the vicinity of the band gap. The optical spectra include a polynomial line broadening of 0.5 eV.

III. RESULTS

A. Path (i): Inward migration

The characteristic energies E^a and ΔE for inward migration of oxygen are summarized in Table I. Migration in the case of an uncharged, fully hydrogenated cluster ($X=Y=$H) is activated by 4.0 eV, which is slightly greater than that obtained previously[19] at 3.5 eV. However, the difference is most likely a consequence of the highly constrained nature of the previous calculations. The positive value of $\triangle E$ is related to the increase in strain energy upon insertion of oxygen into the subsurface, and it is consistent with a thermodynamic driving force for segregation of O to the Si-QD surface where the energy cost of the local structural distortions is lower.

We note that the immediate proximity of hydroxyl groups reduces E^a, but the barriers remain high at around 3 eV, and well above a value where reactions would proceed at room temperature. More significantly, charging leads to greatly reduced barriers: in the positive charge state, the barrier falls from 4.0 to 1.0 eV, although the reaction remains endothermic so that the reverse process is even more favorable. The reduction in E^a for charged systems is due to the breaking of an interlayer Si—Si bond while simultaneously forming a threefold coordinated oxygen atom (labeled TCO), a structure that is similar to the well-known y-lid system.[33] In contrast, this route is not available in a charge-neutral migration process, where the interlayer Si—Si bond has to be broken before subsequent insertion of the oxygen atom.

TABLE I. Activation energies (E^a) and energy changes (ΔE) for inward migration along path (i), Fig. 2, as a function of terminating species and charge state (eV).

Site			0		+1		−1	
X	Y	Z	E^a	ΔE	E^a	ΔE	E^a	ΔE
H	H	H	4.0	0.3	1.0	0.3	1.6	0.3
H	OH	H	3.0	0.3	1.1	0.4	1.6	0.2
OH	OH	H	3.1	0.6	1.1	0.6	1.2	0.4
DB	H	H	2.0	0.3	2.5	0.0	2.0	−0.2
DB	OH	H	1.9	0.3	2.4	0.0	2.0	−0.2
DB	DB	H	1.6	−0.3	1.5	0.0	1.6	0.3
H	H	DB	3.7	0.2	3.5	0.3	3.7	0.2
H	OH	DB	3.9	0.3	3.7	0.3	3.7	0.3
OH	OH	DB	3.2	0.5	3.2	0.5	3.1	0.6
DB	DB	DB	1.9	0.3	2.1	0.6	2.0	0.0

In order to assess the likelihood of the charging of these clusters, we have calculated the adiabatic IP and EA for the systems shown in the first three rows of Table I and found them to lie in the range of -5.7 ± 0.1 and -2.3 ± 0.1 eV, respectively. This may be rather high for thermal ionization, but athermal photoionization may occur, and we note that solvation or the presence of electrochemical processes, neither of which is considered here, could considerably affect these values.

We now turn to systems involving unsaturated sites. A DB at X reduces E^a relative to the analogous fully passivated systems. However, the values (Table I) remain large on a thermal scale and the reactions are endothermic. A surface dangling bond acts both as an electron and hole trap, so that charged systems involving DBs largely behave as the neutral cases. In particular and in contrast to a full passivated system, ionizing the Si-QDs does not reduce E^a.

When a second DB is present at Y, a reduction in E^a is seen for all charge states. We conclude that multiple dangling bonds in the vicinity of the migration pathway aid inward diffusion processes, as noted previously by Hoshino and Nishioka.[19]

For neutral systems, a DB at the distant site Z, where sites X and Y are passivated, results in barriers similar to those where Z is H. For example, $X=Y=Z=$H yields $E^a=4.0$ eV and $X=Y=$H, $Z=$DB has $E^a=3.7$ eV. Since DBs are electrically active, the presence of such a DB at Z inhibits the ionization of the interstitial oxygen. Then, the reduction in activation energy for $Q=\pm1$ for a fully passivated cluster is lost.

B. Threefold coordinated interlayer oxygen

From the calculations of the migration paths, it is clear that many diffusing systems involve a TCO, either as an intermediate or end-point structure. This structure is of particular interest for processes where there is a partially terminated surface (i.e., one or more DBs). An illustration of the TCO for $X=Y=$DB, $Q=0$ is shown in Fig. 3.

For $Q=+1$, with $X=$DB and Y passivated, we find that an interlayer Si-O-Si divalent oxygen structure is unstable and spontaneously forms the overcoordinated TCO system. This is also the case for $Q=0$ and $Q=+1$ where X and Y are DBs. The reaction is either energy neutral or exothermic (see Table I), thermodynamically promoting the movement of oxygen from the surface to the subsurface.

In contrast to our prediction for the stability of the TCO over the interlayer site, previous modeling[19] for a charge-neutral, unterminated surface suggested that the TCO structure was ~0.1 eV *higher* in energy. This then represented an intermediate state for oxygen migration from the surface into the core. However, we note that the TCO is stabilized by a significant perturbation of the surface, which may have been prevented by the small system size adopted in the earlier study.[19]

Although activation energies for production of the TCO structure are rather high, given its thermodynamic stability, photochemical and other athermal processes may result in its production. We have therefore examined this system in more detail.

We plot in Fig. 4 the electronic structure of the TCO, for the case with DBs at X and Y, $Q=0$, and compare it against

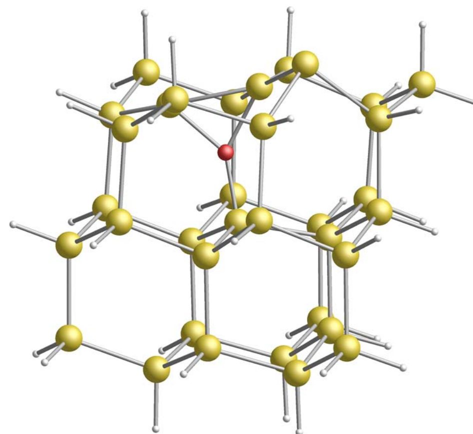

FIG. 3. (Color online) Schematic of the TCO structure $Si_{35}H_{34}O$ with $X=Y=$DB and $Q=0$. Colors as in Fig. 1.

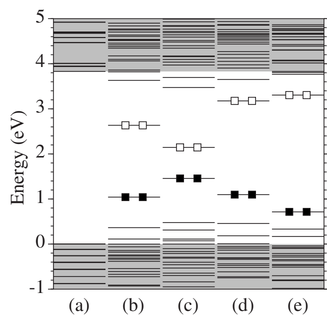

FIG. 4. The Kohn-Sham levels of (a) the oxygen-free, H-terminated Si-QD, (b) Si-QD with DBs at X and Y, (c) Si-QD with DBs at X and Y, oxygen in a Si-O-Si back-bond site, (d) the TCO structure in Fig. 3, and (e) the bridging oxygen structure shown in Fig. 7. Filled and white squares indicate occupied and empty localized levels in the Si-QD gap. The shaded regions indicate the position of the bands for (a).

an oxygen-free, H-terminated Si-QD, an $X=Y=$DB, oxygen-free system, and $X=Y=$DB with oxygen in a surface site rather than the TCO. Figure 4(b) shows that introducing DBs leads to midgap levels, and Fig. 4(c) shows that subsequent introduction of interstitial oxygen pushes the levels deeper into the gap. The restructuring from the surface site into the TCO reverses [Fig. 4(d)], and to first order, the energy reduction (ΔE, Table I) during this reaction can be correlated with the lowering of the occupied gap levels. The localizations of the HOMO and LUMO of the TCO are plotted in Fig. 5. The HOMO shows the stabilizing transfer between a p contribution on the oxygen atom to the dangling bond at site Y.

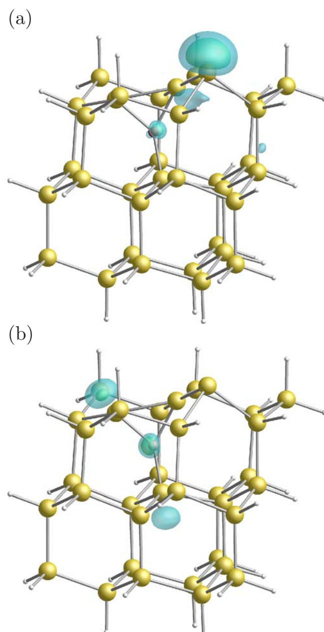

FIG. 5. (Color online) Plots of the wave function squared for the (a) HOMO and (b) LUMO of the TCO structure for $X=Y=$DB in the neutral charge state. These two states represent midgap states relative to the oxygen-free, fully hydrogenated dot.

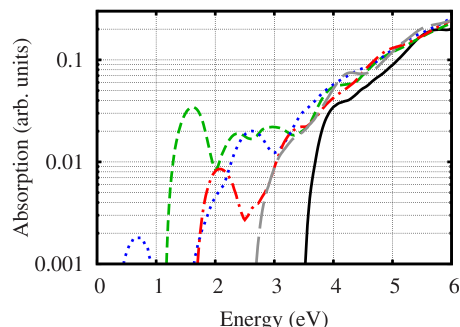

FIG. 6. (Color online) Calculated optical absorption spectra corresponding to the electronic structures plotted in Fig. 4. (a) Black, full line, (b) green, short-dashed line, (c) blue, dotted line, (d) red, dot-dashed line, and (e) gray, long-dashed line.

The presence of filled and empty defect levels in the gap has previously been used as an argument for an emission redshift arising from double-bonded silanone surface groups.[34] The calculated optical absorption for the TCO is shown in Fig. 6. There is a clear redshift of >1.5 eV relative to the pure hydrogen-terminated Si-QD. The optical spectra show midgap transitions between the occupied and empty defect levels, followed by the onset of transitions between the gap levels and band edges, and merge with the optical absorption of the perfect cluster at around 4 eV.

We have also analyzed the vibrational modes associated with the TCO structure and found a localized infrared active Si-O stretch at 769 cm^{-1}, with an additional more localized but probably less intense bending mode at 264 cm^{-1}. To set this into context, we have calculated the vibrational modes associated with surface Si-O-Si and found stretch modes to exist in the range of 930–1010 cm^{-1} dependent on the cluster size and nature of the immediate environment. These results compare well with the experimental value obtained for the asymmetric Si-O stretch mode associated with interstitial oxygen in bulk silicon (1136 cm^{-1}).[35]

C. Path (ii): Lateral migration

As with inward migration, we have tabulated the calculated characteristic energies for lateral migration. Table II shows that for the case of a fully passivated Si-QD, the energetics closely follow those of inward diffusion: the neutral system have higher activation barriers than $Q=\pm1$, and hydroxyl groups modestly reduce the neutral migration barriers.

For systems that include a dangling bond at X, with $Q=0$, the barriers are lowered relative to the comparable fully passivated cases. However, the values are still large. Our calculations indicate that lateral migration with one or no DB is thermally forbidden.

However, in the case of multiple DBs, an additional structure becomes important. In the simulation, the migration is between sites on a (111) facet, and the adsorbed oxygen atom bridges two neighboring dangling bonds. The geometry is shown in Fig. 7, and all atoms have their valence satisfied. This is the same structure reported by Vasiliev *et al.*[16] Al-

TABLE II. Activation energies (E^a) and energy changes (ΔE) for inward migration along path (i), Fig. 2, as a function of terminating species and charge state (eV).

Site			0		+1		−1	
X	Y	Z	E^a	ΔE	E^a	ΔE	E^a	ΔE
H	H	H	3.6	0.0	1.5	0.0	1.8	0.0
H	OH	H	3.4	−0.4	2.0	−0.1	1.5	−0.2
OH	OH	H	2.9	0.0	1.7	0.0	1.5	0.1
DB	H	H	2.3	0.1	2.2	0.4	2.0	−0.4
DB	OH	H	2.0	−0.3	1.9	0.0	2.6	−0.8
DB	DB	H	⋯	⋯	⋯	⋯	0.8	0.0
H	H	DB	3.5	−0.1	3.4	0.0	3.7	0.1
H	OH	DB	3.6	−0.2	3.4	−0.3	2.9	−0.3
OH	OH	DB	3.1	−0.1	3.3	−0.1	2.9	0.2

though there is considerable localized strain as the second-neighbor silicon atoms are pulled together, the chemical stability is sufficient to make the bridging structure energetically favored over oxygen insertion into the silicon backbond network. Preliminary calculations indicate that the bridging site is favored for larger Si-QDs, at least up to Si_{275}, a cluster that corresponds to a Si-QD core diameter of $\sim$2 nm.

Where the bridging site is possible, we find that it represents the most stable configuration for oxygen. The barrier for lateral migration where there are two neighboring DBs is therefore limited by this deep trap. Therefore, migration paths involving $X=Y=$DB are not present in Table II with the exception of $Q=-1$, $X=Y=$DB. The EA calculated for surface oxygen with two DBs is −3.7 eV, making the occurrence of this charge state more likely than for the fully passivated systems and significantly likely on a thermal scale. For this combination, the bridge structure is only metastable, and the barrier is particularly small, suggesting that in the presence of excess electron charge, DBs may enhance the mobility of surface oxygen.

Finally, we note that, as with the TCO, the bridging structure leads to relatively shallow gap levels, as plotted in Fig. 4(e). This yields a redshift in the optical spectrum [gray, long-dashed curve (Fig. 6)] relative to the $Si_{35}H_{36}$ Si-QD. The redshift is a consequence of transitions between the gap states, which are dipole allowed due to the low symmetry. We note that this appears to be in contrast with the conclusions made for the same defect previously.[16] The relative location of the gap levels leads a smaller redshift for the bridging center than calculated for the TCO and DB systems.

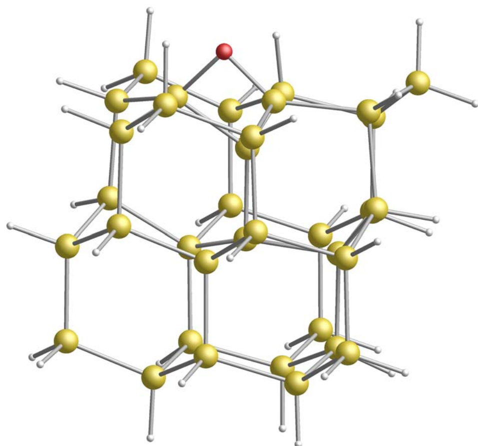

FIG. 7. (Color online) An illustration of the oxygen bridging structure in $Si_{35}H_{34}O$ for $X=Y=$DB, with $Q=0$. Colors as in Fig. 1.

D. Dangling bond migration

We have shown that DBs play a key role in oxygen migration processes, so their mobility is also of interest. We note that the activation energy for diffusion of hydrogen across a clean Si (111)-(7×7) surface has been determined via scanning tunneling microscopy to be 1.69–1.91 eV.[36] We have calculated the activation energy for a similar process on our Si-QD in the three charge states. We find that E^a are 1.7, 2.0, and 1.5 eV for $Q=0$, +1, and −1, respectively, in good agreement with the experiment.

Therefore, in the absence of any catalytic species in the environment, the DBs on (111) facets will be immobile on partially passivated Si-QD surfaces at room temperature, at least for the migration path examined in this study.

IV. CONCLUSIONS

We have performed density functional simulations for selected migration processes of oxygen inward and lateral to the surface of a Si-QD. In general, barriers to migration are in excess of the thermal energy available for room temperature processes. With a few exceptions, the reactions moving oxygen further into the Si-QDs are also endothermic, so that kinetics and thermodynamics both favor oxygen residing in surface Si—Si bonds.

In addition, the activation energy for migration significantly exceeds that determined for bulk silicon. This can be traced to the surface relaxation not available for the bulk. Our results fit well with the observation of self-limiting oxidation[7,8] and weakened oxygen diffusion relative to the bulk.[9]

We have also shown that unsaturated surface sites lower the barrier to inward migration to the immediate subsurface layer, although the barriers remain high on a thermal scale. Multiple dangling bonds lead to highly stable TCO and surface bridging structures. Both of these minima yield gap levels giving rise to redshifts in the onset of optical absorption. The bridging structure on dihydride, (001)-like surface facets have also been characterized as leading to redshifts.[16,17] The calculated activation energy for migration of surface dangling bonds suggests that any enhancement of oxidation due to such sites will only occur when the oxygen centers and DBs are formed in close proximity. For example, this may be the case if hydrogen abstraction occurs from a Si atom bonded to a surface back-bonded interstitial oxygen.

Finally, the IP and EA of this 1 nm Si-QD suggest that charging is most likely where surface DBs are present. Under these circumstances, the charging may lead to an enhance lateral migration of oxygen, but inward diffusion is generally thermodynamically unfavorable.

ACKNOWLEDGMENTS

We gratefully thank Ben Horrocks for useful discussions and the EPSRC UK for financial support.

*r.j.eyre@ncl.ac.uk

[1] A. Puzder, A. J. Williamson, J. C. Grossman, and G. Galli, Phys. Rev. Lett. **88**, 097401 (2002).

[2] M. V. Wolkin, J. Jorne, P. M. Fauchet, G. Allan, and C. Delerue, Phys. Rev. Lett. **82**, 197 (1999).

[3] I. Umezu, T. Kimura, and A. Sugimura, Physica B **376-377**, 853 (2006).

[4] K. Shinoda, S. Yanagisawa, K. Sato, and K. Hirakuri, J. Cryst. Growth **188**, 84 (2006).

[5] F. Hua, F. Erogbogbo, M. T. Swihart, and E. Ruckenstein, Langmuir **22**, 4363 (2006).

[6] Y. Chao, A. Houlton, B. R. Horrocks, M. R. C. Hunt, N. R. J. Poulton, J. Yang, and L. Siller, Appl. Phys. Lett. **88**, 263119 (2006).

[7] H. Hofmeister, F. Huisken, and B. Kohn, Eur. Phys. J. D **9**, 137 (1999).

[8] G. Ledoux, J. Gong, and F. Huisken, Appl. Phys. Lett. **79**, 4028 (2001).

[9] D.-Q. Yang, J.-N. Gillet, M. Meunier, and E. Sacher, J. Appl. Phys. **97**, 024303 (2005).

[10] X. D. Pi, L. Mangolini, S. A. Campbell, and U. Kortshagen, Phys. Rev. B **75**, 085423 (2007).

[11] H. Ikeda, K. Hotta, T. Yamada, S. Zaima, H. Iwano, and Y. Yasuda, J. Appl. Phys. **77**, 5125 (1995).

[12] K. Sato, Y. Nakagawa, H. Ikeda, S. Zaima, and Y. Yasuda, Thin Solid Films **369**, 277 (2000).

[13] E. Froner, R. Adamo, Z. Gaburro, B. Margesin, L. Pavesi, A. Rigo, and M. Scarpa, J. Nanopart. Res. **8**, 1071 (2006).

[14] E. P. Boonekamp, J. J. Kelly, J. van de Ven, and A. H. M. Sondag, J. Appl. Phys. **75**, 8121 (1994).

[15] G. Rao, Z.-H. Wang, H. Watanabe, M. Aoyagi, and T. Urisu, Surf. Sci. **570**, 178 (2004).

[16] I. Vasiliev, J. R. Chelikowsky, and R. M. Martin, Phys. Rev. B **65**, 121302(R) (2002).

[17] M. Nishida, Phys. Rev. B **69**, 165324 (2004).

[18] L. E. Ramos, J. Furthmuller, and F. Bechstedt, Phys. Rev. B **70**, 033311 (2004).

[19] T. Hoshino and Y. Nishioka, Phys. Rev. B **64**, 125322 (2001).

[20] G. D. Watkins, J. W. Corbett, and R. S. McDonald, J. Appl. Phys. **53**, 7097 (1982).

[21] J. C. Mikkelsen, Jr., in *Oxygen, Carbon, Hydrogen and Nitrogen in Crystalline Silicon*, edited by J. C. Mikkelsen, Jr., J. W. Corbett, and S. J. Pennycook, MRS Symposia Proceedings No. 59 (Materials Research Society, Pittsburgh, 1986), p. 19.

[22] Z. Jiang and R. A. Brown, Phys. Rev. Lett. **74**, 2046 (1995).

[23] M. Ramamoorthy and S. T. Pantelides, Phys. Rev. Lett. **76**, 267 (1996).

[24] J. P. Perdew, K. Burke, and M. Ernzerhof, Phys. Rev. Lett. **77**, 3865 (1996).

[25] R. Jones and P. R. Briddon, in *Identification of Defects in Semiconductors*, edited by M. Stavola, Semiconductors and Semimetals Vol. 51A (Academic, Boston, 1998), Chap. 6.

[26] C. Hartwigsen, S. Goedecker, and J. Hutter, Phys. Rev. B **58**, 3641 (1998).

[27] J. P. Goss, M. J. Shaw, and P. R. Briddon, in *Theory of Defects in Semiconductors*, edited by David A. Drabold and Stefan K. Estreicher, Topics in Applied Physics Vol. 104 (Springer, Berlin, 2007), pp. 69–94.

[28] G. Henkelman, B. P. Uberuaga, and H. Jónsson, J. Chem. Phys. **113**, 9901 (2000).

[29] G. Henkelman and H. Jónsson, J. Chem. Phys. **113**, 9978 (2000).

[30] F. Cichos, J. Martin, and C. von Borczyskowski, Phys. Rev. B **70**, 115314 (2004).

[31] I. Sychugov, R. Juhasz, J. Linnros, and J. Valenta, Phys. Rev. B **71**, 115331 (2005).

[32] C. J. Fall, A. T. Blumenau, R. Jones, P. R. Briddon, T. Frauenheim, A. Gutiérrez-Sosa, U. Bangert, A. E. Mora, J. W. Steeds, and J. E. Butler, Phys. Rev. B **65**, 205206 (2002).

[33] M. Saito and A. Oshiyama, Phys. Rev. B **38**, 10711 (1988).

[34] A. Puzder, A. J. Williamson, J. C. Grossman, and G. Galli, J. Chem. Phys. **117**, 6721 (2002).

[35] H. J. Hrostowski and R. H. Kaiser, Phys. Rev. **107**, 966 (1957).

[36] R.-L. Lo, I.-S. Hwang, M.-S. Ho, and T. T. Tsong, Phys. Rev. Lett. **80**, 5584 (1998).